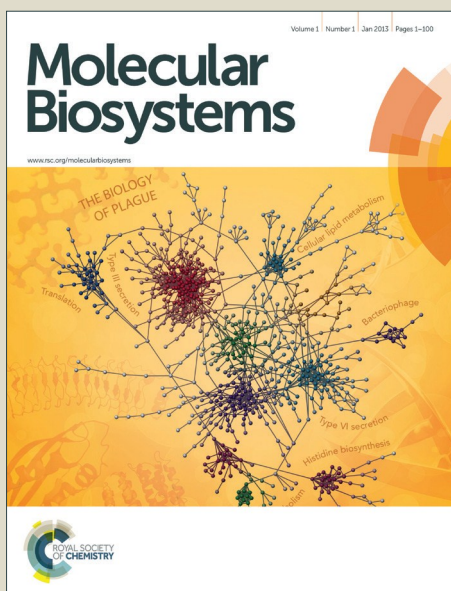


# Molecular BioSystems

Accepted Manuscript



This is an *Accepted Manuscript*, which has been through the Royal Society of Chemistry peer review process and has been accepted for publication.

*Accepted Manuscripts* are published online shortly after acceptance, before technical editing, formatting and proof reading. Using this free service, authors can make their results available to the community, in citable form, before we publish the edited article. We will replace this *Accepted Manuscript* with the edited and formatted *Advance Article* as soon as it is available.

You can find more information about *Accepted Manuscripts* in the [Information for Authors](#).

Please note that technical editing may introduce minor changes to the text and/or graphics, which may alter content. The journal's standard [Terms & Conditions](#) and the [Ethical guidelines](#) still apply. In no event shall the Royal Society of Chemistry be held responsible for any errors or omissions in this *Accepted Manuscript* or any consequences arising from the use of any information it contains.



[www.rsc.org/molecularbiosystems](http://www.rsc.org/molecularbiosystems)

## A quinazoline-based HDAC inhibitor affects gene expression pathways involved in cholesterol biosynthesis and mevalonate in prostate cancer cells.

Z. Lin<sup>1</sup>, K. S. Bishop<sup>1\*</sup>, H. Sutherland<sup>1</sup>, G. Marlow<sup>2</sup>, P. Murray<sup>1</sup>, W. A. Denny<sup>1</sup> and L.R. Ferguson<sup>1,2</sup>

<sup>1</sup> Auckland Cancer Society Research Centre, University of Auckland, New Zealand

<sup>2</sup> Discipline of Nutrition and Dietetics, University of Auckland, New Zealand.

\*Corresponding author.

### Abstract

Chronic inflammation can lead to the development of cancers and resolution of inflammation is an ongoing challenge. Inflammation can result from dysregulation of the epigenome and a number of compounds that modify the epigenome are in clinical use. In this study the anti-inflammatory and anti-cancer effects of a quinazoline epigenetic-modulator compound were determined in prostate cancer cell lines using a non-hypothesis driven transcriptomics strategy utilising the Affymetrix PrimeView<sup>®</sup> Human Gene Expression microarray. GATHER and IPA software were used to analyse the data and to provide information on significantly modified biological processes, pathways and networks. A number of genes were differentially expressed in both PC3 and DU145 prostate cancer cell lines. The top canonical pathways that frequently arose across both cell lines at a number of time points included cholesterol biosynthesis and metabolism, and the mevalonate pathway. Targeting of sterol and mevalonate pathways may be a powerful anticancer approach.

Keywords: transcriptomics, Affymetrix, HDAC inhibitor, cholesterol biosynthesis, mevalonate pathway, prostate cancer.

### 1. Introduction

Although inflammation is a necessary immune response, chronic inflammation can lead to the development of cancers as well as other chronic diseases, and there are ongoing efforts to either block pro-inflammatory mediators or to stimulate resolution of inflammation.<sup>1</sup> Deregulation of the epigenome can result in a range of chronic diseases associated with inflammation, and a number of compounds that modify the epigenome are in clinical use today.<sup>2</sup>

Chromatin remodelling plays a key role in gene expression, and epigenetic modifications may be as important as mutations, insertions and deletions in tumour development and progression.<sup>3</sup> Unlike genetic mutations, epigenetic changes that have resulted in gene activation or silencing can sometimes be reversed by small molecules that modify the epigenome. One such group of small molecules are the histone deacetylase (HDAC) inhibitors. HDACs influence the expression of a number of key enzymes involved in pathways associated with apoptosis, cell cycle, tumour cell proliferation and inflammation, amongst others<sup>4</sup> and tumour progression is associated with an increase in HDAC activity.<sup>5</sup> However, although HDAC inhibitors have an impact on tumour and T cell lymphomas rather than non-malignant cells, their mechanism of action remains unclear.<sup>4</sup>

HDACs and histone acetyltransferases (HATs) act in opposition to modify chromatin and thus control gene expression.<sup>6</sup> HDACs can repress transcription by bringing about chromatin condensation in response to the removal of acetyl groups from histone tails.<sup>6</sup> Not only have HDACs been found to be aberrantly recruited to "inappropriate" loci, but abnormal expression of HDACs 1, 2, 3 and 6 have been reported in numerous types of cancer e.g. gastric, breast, prostate, colorectal and cervical.<sup>6</sup> SN30028 is an HDAC inhibitor that was identified from an in-house compound library.<sup>7</sup> SN30028 (Figure 1) is

regarded as a quinazoline drug and was selected from the aforementioned compound library based on its anti-inflammatory activity and the strength of HDAC inhibition.<sup>7,8</sup>

SN30028 decreased the activity of HDAC 1, 3 and 6 by 23%, 76% and 48% respectively.<sup>9</sup> HDACs 1 and 3, HDAC class I compounds, are restricted to the nucleus and are believed to play a key role in cell survival and proliferation.<sup>10</sup> Loss of HDAC 1 activity results in an overall reduction of deacetylase activity, reduced proliferation rates and increased levels of the cyclin-dependent kinase inhibitors p21 and p27.<sup>11</sup> HDAC 3 is important as it mediates gene expression of tumour necrosis factor (TNF) as well as the expression of other genes.<sup>12</sup>

HDAC 6 belongs to the HDAC Class 2b group of compounds and is unique as it has two catalytic domains and a zinc finger.<sup>6</sup> HDAC 6 is of interest as it helps to protect against cellular stress by the regulation of heat shock protein 90 and alpha tubulin and down-regulation can bring about apoptosis and inhibition of metastasis.<sup>13,14</sup>

Determining the effect of a particular compound on cancer cell lines can be challenging as effects on any one gene can be small, and these effects can also be broad. For this reason the anti-inflammatory and anti-cancer effects of a quinazoline epigenetic-modulator compound were determined, in prostate cancer cell lines, using a transcriptomics approach.

One advantage of transcriptomics is that experimental design is non-hypothesis driven, and provides sufficient sensitivity and breadth to examine the expression of thousands of genes simultaneously.<sup>15</sup> The Affymetrix PrimeView GeneChip Human Microarray was used as it is a “perfect-match-only” (probe to transcript) array<sup>16</sup> and therefore the false signal changes referred to by Li *et al*<sup>17</sup> are less likely to arise.

In addition biological processes are likely to be represented by complex networks consisting of multiple signalling modules rather than a series of linear pathways<sup>18</sup> and thus a transcriptomics approach, followed by network analysis, was deemed preferable. The aim of this study was to determine the effect of SN30028 on differential gene expression in prostate cancer cell lines with a particular focus on inflammation and epigenetic modulation. Compounds, that restore histone acetylation, have potential as anti-inflammatory and anti-cancer drugs<sup>19</sup>, and we show evidence that the known<sup>7</sup> quinazoline-based HDAC inhibitor SN30028 (Figure 1) influenced cholesterol biosynthesis and mevalonate pathways.

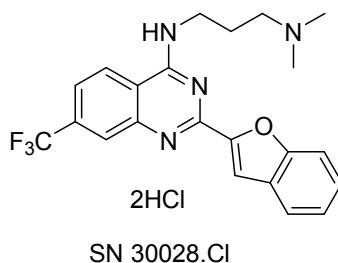


**Figure 1.** Chemical structure of SN30028

## 2. Methods

### 2.1 Cell culture

The prostate cancer cell lines PC3, DU145 and LNCaP were obtained from the American Type Culture Collection (VA, USA) and maintained in Alpha 5 minimum essential media (Gibco, Invitrogen Corporation, New York, USA) with 10% fetal calf serum (Morgate Biotech, Hamilton, New Zealand) and 100 IU penicillin/streptomycin (Sigma Chemical Company, St Louis, MO, USA). Cells were cultured in a water jacketed incubator (Thermo Fisher Scientific, MA, USA) at 37°C with 5% CO<sub>2</sub>, and passaged twice weekly. The 50% inhibitory concentrations (IC50s) for SN30028 and a number of other compounds were established and the anti-proliferative activity was determined relative to the reference drugs suberoylanilide hydroxamic acid (SAHA) (Sigma Chemical Company, St Louis, MO, USA) and 5'-aza-2-deoxycytidine (Sigma-Aldrich, St Louis, MO, USA). Dimethyl sulphoxide (DMSO) (Merck, Darmstadt, Germany) was used as a solvent for the compounds tested and hence was also used as a control. The IC50s were performed on PC3, DU145 and LNCaP using the sulforhodamine B colourimetric assay.<sup>20</sup> Three independent experiments were performed in quadruplicate.

### 2.2 HDAC Activity

HDAC activity was assessed from total protein extracted from DU145, PC3 and LNCaP cells following treatment for 24 hours with a number of compounds (TSA, SAHA, SN30028, SN30029, SN30140, SN29887, SN29984, SN30711, 5-aza-2-deoxycytidine (5AZA) (Sigma Aldrich, St Louis, USA) at their respective IC50 concentrations. Total protein was extracted from each treated cell line grown in P100 plates. The cells were washed with PBS, lysed (lysis buffer containing 1% Triton X-100 (Sigma Aldrich, St Louis, USA), frozen, then thawed and removed to a micro-centrifuge tube, whereupon the cells were centrifuged and the supernatant collected. Protein concentration was assessed using the bicinchoninic acid (Sigma Aldrich, St Louis, USA) protein assay (as outlined in Lin *et al.*).<sup>7</sup>

Using the manufacturer's protocol the HDAC Fluorometric Activity Assay (BIOMOL International – Cayman Chemical, Ann Arbor, USA) was used to measure the effect of compounds on HDAC activity from the extracted protein. Three independent experiments were performed in duplicate.

### 2.3 Transcriptomics

Two prostate cancer cell lines, namely DU145 and PC3 cells, were treated with SN30028 and harvested at 4, 24 and 96 hours after dosing (Figure 2). In addition, cell lines were incubated with an equivalent amount of water for each of the three time points. These served as controls. DU145 and PC3 were chosen ahead of LNCaP as the aforementioned were shown to have greater sensitivity to HDAC inhibition than LNCaP<sup>9</sup> (see section 3.1) A QIAshredder (Qiagen, MD, USA) was used to disrupt the cells and an RNeasy Mini kit (Qiagen, MD, USA) was used to isolate the RNA in triplicate, following the manufacturer's recommended protocol. The quantity and quality of RNA was determined using the NanoDrop ND 1000 spectrophotometer (NanoDrop Technologies, Wilmington, USA) and the Experion RNA StdSens Analysis Kit (Biorad, Hercules, USA) respectively. Approximately 500ng of RNA with a RIN value of  $\geq 8$  were required for the PrimeView<sup>®</sup> Human Gene Expression arrays (Affymetrix, CA, USA). The RNA was reverse transcribed, biotin labelled, fragmented, hybridised to the gene chip and scanned<sup>21</sup> by the Centre for Genomics and Proteomics (New Zealand Genomics Ltd., University of Auckland, New Zealand).

The PrimeView<sup>®</sup> Human Gene Expression array uses 530 000 probes covering 36 000 transcripts and variants located in more than 20 000 genes<sup>22</sup>. Transcripts were measured independently by using multiple probes. The level of gene expression was associated with the probe/s targeting that specific gene and following adjustment for the solvent/media controls, differential gene expression was calculated. The workflow for the analysis of the gene expression array data is outlined in Figure 2.

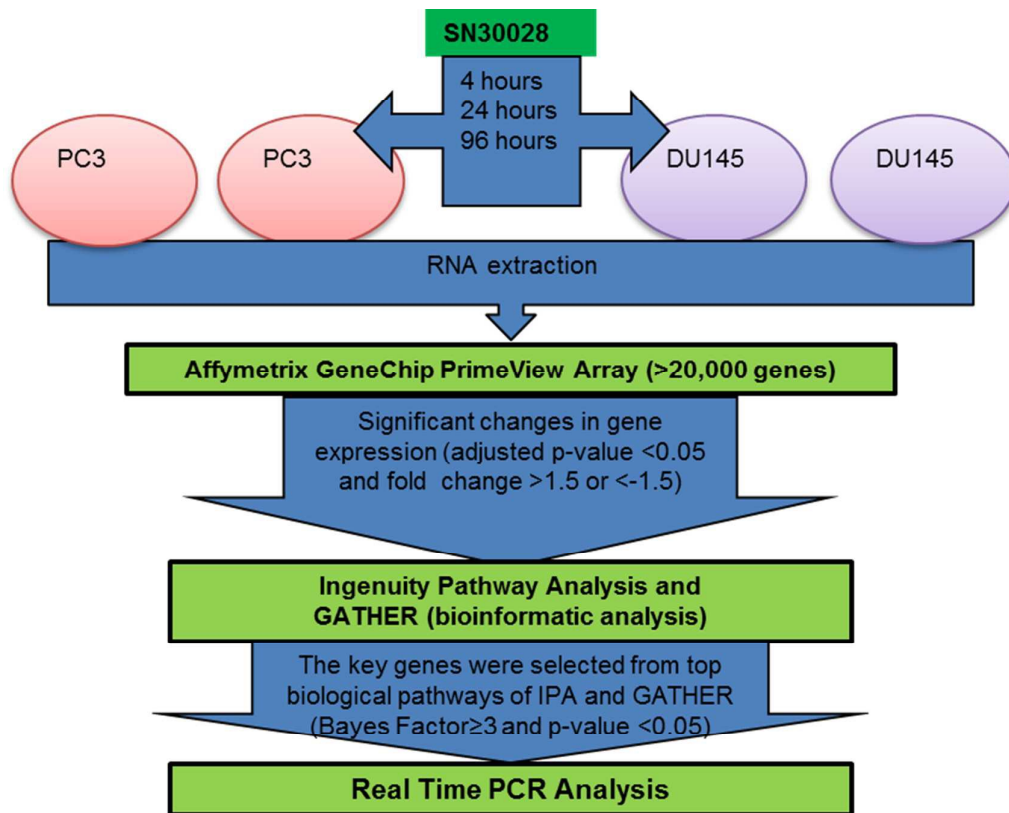


**Figure 2.** Workflow for microarray analysis of differential gene expression generated from prostate cancer cells treated with SN30028 (<sup>9</sup> adapted from <sup>23</sup>).

Confirmation of the microarray results was carried out using quantitative reverse transcription polymerase chain reaction (qRT-PCR) and 27 statistically significant differentially expressed genes were selected for validation. The 27 TaqMan probe sets were obtained from ThermoFisher (Pleasanton, USA). The aforementioned RNA (section 2.2) was isolated from DU145 and PC3 following treatment for 4 and 24hrs, converted to cDNA using a Quantitect Reverse Transcription Kit (Qiagen, Victoria, Australia) and PCR was performed (on the three biological repeats as well as non-template controls) on an Applied Biosystems 7900 thermocycler (Waltham, USA). *Glyceraldehyde-3-phosphate dehydrogenase (GAPDH)*, *hypoxanthine phosphor-ribosyltransferase 1 (HPRT1)*, and *β-actin (ACTB)* were tested for assessment as normalisation genes for RNA expression. A standard curve was calculated from technical triplicates using SDS2.3 and RQ Manager 2.2 software (Applied Biosystems, USA). The relative expression of each of the genes was calculated as fold change using a delta delta cycle threshold (Ct) method.<sup>24</sup> Thereafter fold changes from the Affymetrix and qRT-PCR experiments were compared.

## 2.4 Data analysis

To identify the differentially expressed genes, the data from the microarray experiments were subjected to Robust Multiarray Analysis<sup>25</sup> to assess for quantile normalisation and then filtered based on the following parameters: (adjusted p value  $\leq 0.05$ ; fold change  $\geq 1.5$ ). The “Limma” package within the statistical language R<sup>26</sup> was used to analyse the CEL files generated by the Affymetrix GeneChip Instrument System (Affymetrix, MD, USA). Gene expression values were based on the absorbance values of the probes targeting each specific gene. Changes in average gene expression in response to treatment were calculated as fold changes. P-values were calculated so as to determine whether the changes in gene expression were significant (Figure 2). A multiple testing correction was applied using Benjamini-Hochberg’s false-discovery rate<sup>27</sup> set at 5%. Functional, pathway and network analyses were performed by using GATHER (Gene Annotation Tool to Help Explain Relationships<sup>28</sup>) and IPA (Ingenuity Pathway Analysis<sup>29</sup>) software. Networks were ranked by a score that was assigned based on the probability that a collection of nodes within that network can occur by chance. A number of networks scored highly, but only the highest scoring network per cell line – treatment time combination were presented here so as to avoid biasing results through “fishing” (Supplementary Figures 1-6). The network score indicates the likelihood of Focus Genes in a network being found together, and it is clear from the high scores that one should be confident that these associations were not generated by chance.<sup>30</sup> IPA constructs networks using a stepwise process. Networks are constructed in such a way that both interconnectivity between Focus Genes and the number of Focus Genes in the network are optimised (using a network size of 35 or 70 genes/proteins, as specified in the figure legends).

## 3 Results

The four day IC<sub>50</sub> concentrations were established for PC3, DU145 and LNCaP cell lines and the results are listed in Table 1.

Table 1. Dosages required to achieve IC<sub>50</sub>s for PC3, DU145 and LNCaP cells following four days of treatment with novel and control compounds.

Compounds ( $\mu\text{M}$ )	PC3	DU145	LNCaP
	IC <sub>50</sub>	IC <sub>50</sub>	IC <sub>50</sub>
SN30028	4.58	7.30	0.82
SN30029	2.87	3.82	0.84
SN30140	2.31	3.9	0.71
SN29887	3.61	12.7	6.92
SN29984	7.13	15.66	6.38
SN26855	1.65	0.49	1.11
SAHA	0.88	0.92	0.58
5'-aza-2-deoxycytidine	0.25	0.31	0.53

SAHA = suberoylanilide hydroxamic acid

With the exception of SN26855, DU145 cells showed the greatest tolerance to the novel compounds tested. In general, LNCaP cells appeared to be the most sensitive to the novel compounds.

### 3.1 HDAC inhibition

Following treatment of cells for 24hrs, total protein was extracted. The effects of compounds of interest on HDAC activity are shown in Figures 3 -5. The HDAC activity of total protein extracted from the cell lines, varied from one cell line to another and varied amongst the novel compounds. HDAC activity of DU145 cells was markedly reduced following

treatment with all the novel compounds, particularly SN30028 (Figure 4.), whilst SN30140 had the largest reduction in HDAC activity in PC3 cells (Figure 3.). The novel compounds did not appear to reduce HDAC activity in LNCaP cells (Figure 5.).

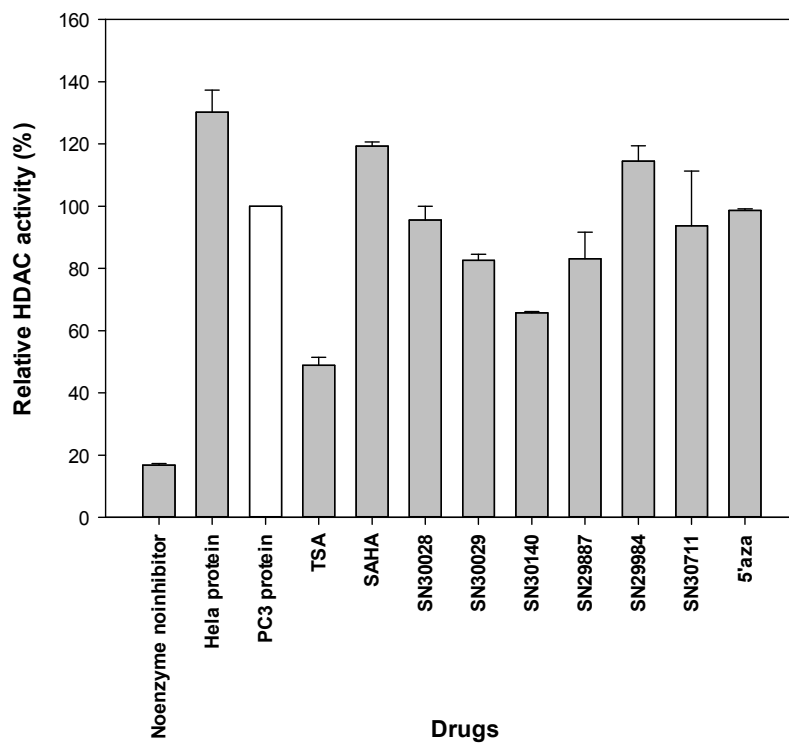


Figure 3. Effect of selected compounds on HDAC activity in PC3 cells

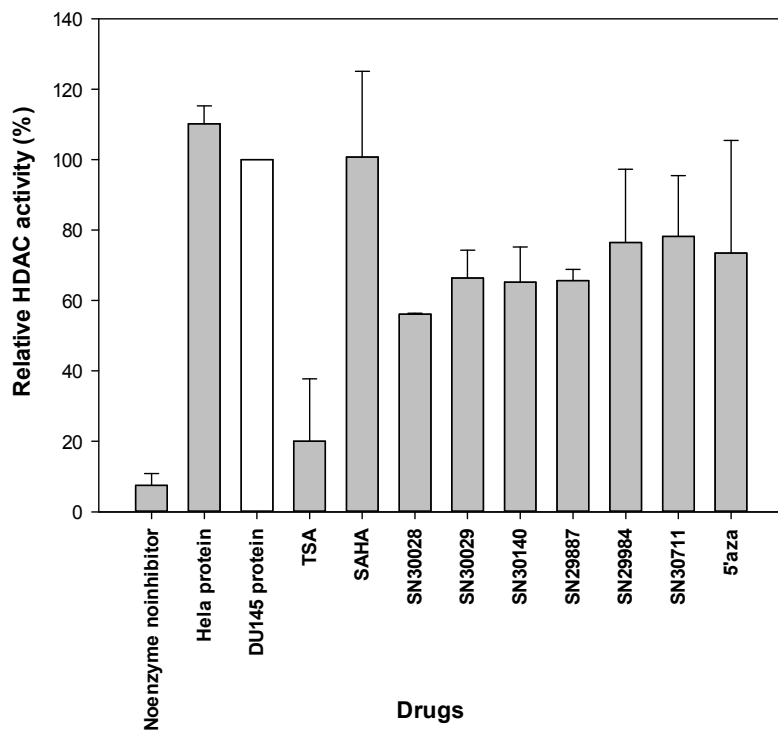


Figure 4. Effect of selected compounds on HDAC activity in total protein extracted from DU145 cells.



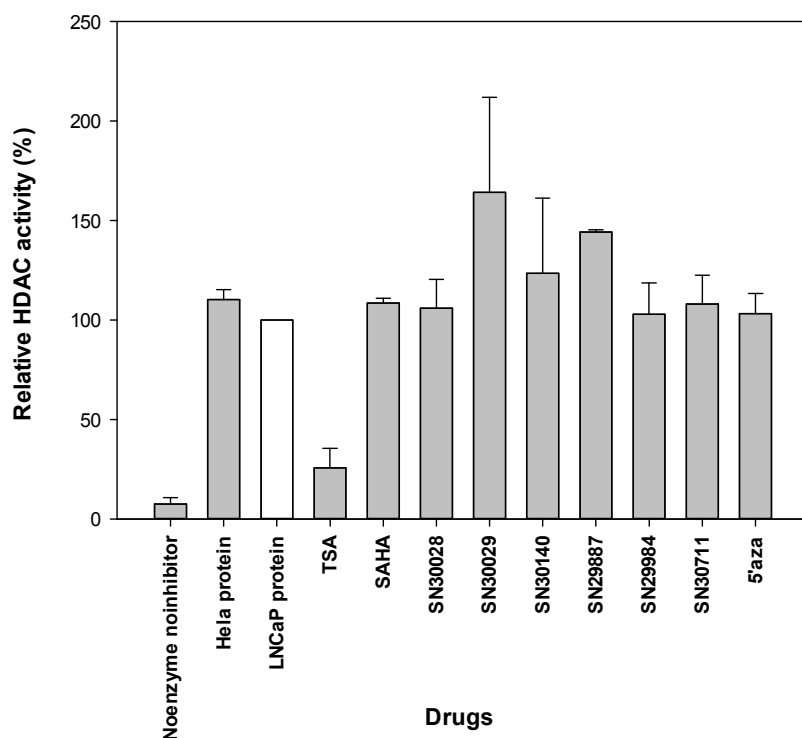


Figure 5. Effect of selected compounds on HDAC activity in total protein extracted from LNCaP cells.

### 3.2 Differential Gene Expression (Affymetrix PrimeView™ Microarrays)

Following the analysis of the Affymetrix PrimeView™ microarray data, it was found that a number of genes in PC3 and DU145 were differentially expressed ( $p \leq 0.05$ ; fold change  $\geq 1.5$ ) following treatment with SN30028. In total 59, 7 and 64 genes were up-regulated and 38, 6 and 34 genes were down-regulated in PC3 at 4, 24 and 96 hours respectively. In DU145 49, 108 and 796 genes were up-regulated and 3, 4 and 399 genes were down-regulated at 4, 24 and 96 hours respectively. A list of ten of the most differentially expressed genes for each cell line–time point combination, with statistically significant p-values and a fold change of  $\geq 1.5$  are shown in Tables 2 (PC3) and 3 (DU145). The genes listed in the table were selected based on the absolute fold change and presented from largest to smallest, regardless of the direction of change.

Table 2. The top ten differentially expressed genes following SN30028 treatment of PC3 cells for 4, 24 and 96 hours.

Cell line Time	Gene symbol	Gene Name	Fold change	p-value ( $\leq$ )
PC3 4 hours	MMP3	matrix metalloproteinase 3 (stromelysin 1, progelatinase)	2.25	2.00E-05
	HEXA	hexosaminidase A (alpha polypeptide)	-2.17	1.07E-02
	CSF2	colony stimulating factor 2 (granulocyte-macrophage)	2.16	3.00E-04
	CYP1B1	cytochrome P450, family 1, subfamily B, polypeptide 1	-2.03	9.20E-04
	PHC1	polyhomeotic homolog 1 (Drosophila)	-1.96	1.50E-04
	PNRC1	proline-rich nuclear receptor coactivator 1	1.91	3.30E-04
	VNN1	vanin 1	1.87	7.00E-05

	RAB5C	RAB5C, member RAS oncogene family	1.86	1.06E-03
	SNORA28	small nucleolar RNA, H/ACA box 28	-1.73	6.40E-04
	SPEN	spen homolog, transcriptional regulator (Drosophila)	-1.73	1.85E-02
PC3 24 hours	PTGS2	prostaglandin-endoperoxide synthase 2 (prostaglandin G/H synthase and cyclooxygenase)	-2.47	4.34E-02
	EPGN	epithelial mitogen homolog (mouse)	-2.26	4.16E-02
	CYP1B1	cytochrome P450, family 1, subfamily B, polypeptide 1	-2.07	1.25E-02
	RGS4	regulator of G-protein signalling 4	1.98	4.34E-02
	AREG	amphiregulin	-1.87	3.80E-02
	GULP1	GULP, engulfment adaptor PTB domain containing 1	1.83	4.10E-02
	SC4MOL	sterol-C4-methyl oxidase-like	1.76	1.12E-02
	SGK2	serum/glucocorticoid regulated kinase 2	-1.76	1.85E-02
	RNF144A	ring finger protein 144A	1.75	1.25E-02
	KRT17	keratin 17	-1.71	4.16E-02
PC3 96 hours	SCNN1G	sodium channel, non-voltage-gated 1, gamma	2.92	1.72E-02
	DDIT3	DNA-damage-inducible transcript 3	-2.77	4.57E-02
	CXCR7	chemokine (C-X-C motif) receptor 7	2.49	3.12E-02
	CHRNA1	cholinergic receptor, nicotinic, alpha 1 (muscle)	2.38	2.13E-02
	HERPUD1	homocysteine-inducible, endoplasmic reticulum stress-inducible, ubiquitin-like domain member 1	-2.11	3.67E-02
	STC1	stanniocalcin 1	2.10	4.22E-02
	TMSB15A	thymosin beta 15a	2.04	2.40E-02
	HSPA5	heat shock 70kDa protein 5 (glucose-regulated protein, 78kDa)	-2.04	2.86E-02
	SESN2	sestrin 2	-1.98	3.12E-02
AREG	amphiregulin	-1.95	3.12E-02	

Table 3. The top ten differentially expressed genes following SN30028 treatment of DU145 cells for 4, 24 and 96 hours.

Cell line Time	Gene symbol	Gene Name	Fold change	p-value ( $\leq$ )
DU145 4 hours	INSIG1	insulin induced gene 1	2.74	2.03E-02
	ULBP1	UL16 binding protein 1	2.24	2.02E-03
	HMGCS1	3-hydroxy-3-methylglutaryl-CoA synthase 1 (soluble)	2.17	3.71E-02
	DDIT4	DNA-damage-inducible transcript 4	2.07	2.03E-02
	BDP1	B double prime 1, subunit of RNA polymerase III transcription initiation factor IIIB	2.06	3.00E-02
	SC4MOL	sterol-C4-methyl oxidase-like	2.01	2.03E-02
	LPIN1	lipin 1	1.95	5.55E-03
	EGFR	epidermal growth factor receptor	1.94	3.53E-02
	CEP350	centrosomal protein 350kDa	1.91	2.29E-02
	MLL3	myeloid/lymphoid or mixed-lineage leukemia 3	1.89	1.24E-02
DU145 24 hours	IFIT2	interferon-induced protein with tetratricopeptide repeats 2	3.09	2.23E-03
	HMGCS1	3-hydroxy-3-methylglutaryl-CoA synthase 1 (soluble)	3.02	9.05E-03
	SC4MOL	sterol-C4-methyl oxidase-like	3.01	4.72E-04
	IFIT3	interferon-induced protein with tetratricopeptide repeats	2.98	1.34E-02

		3		
	INSIG1	insulin induced gene 1	2.89	2.14E-03
	IFIT1	interferon-induced protein with tetratricopeptide repeats 1	2.82	4.72E-04
	AKR1B10	aldo-keto reductase family 1, member B10 (aldose reductase)	2.58	2.21E-03
	IFI44	interferon-induced protein 44	2.52	1.71E-02
	OASL	2'-5'-oligoadenylate synthetase-like	2.44	4.72E-04
	DDX60	DEAD (Asp-Glu-Ala-Asp) box polypeptide 60	2.41	5.30E-03
DU145	MMP1	matrix metalloproteinase 1 (interstitial collagenase)	7.00	8.28E-06
96 hours	S100A9	S100 calcium binding protein A9	-5.47	1.96E-04
	IGFBP3	insulin-like growth factor binding protein 3	-5.41	2.92E-05
	C3	complement component 3	-4.79	7.94E-05
	SLPI	secretory leukocyte peptidase inhibitor	-4.51	3.21E-04
	GKN2	gastrokine 2	4.50	9.97E-06
	AKR1C1	aldo-keto reductase family 1, member C1 (dihydrodiol dehydrogenase 1; 20-alpha (3-alpha)-hydroxysteroid dehydrogenase)	-4.47	1.04E-03
	CDH1	cadherin 1, type 1, E-cadherin (epithelial)	-4.39	1.69E-04
	CYP4F11	cytochrome P450, family 4, subfamily F, polypeptide 11	-4.08	2.99E-04
	AKR1C1/// R1C2	aldo-keto reductase family 1, member C1 (dihydrodiol dehydrogenase 1; 20-alpha (3-alpha)-hydroxysteroid dehydrogenase) /// aldose reductase family 1, member C2 (dihydrodiol dehydrogenase 2; bile acid binding protein; 3-alpha hydroxysteroid dehydrogenase)	-4.06	1.12E-03

### 3.3 Validation of the differential gene expression data generated by Affymetrix PrimeView™ microarray

To corroborate the differential gene expression data generated by the Affymetrix assay a validation was undertaken by comparing the aforementioned data with that obtained from a select number of genes tested using qRT-PCR. qRT-PCR is widely used for accurate expression profiling of key genes<sup>31</sup> and is a suitable technique to validate differential gene expression data generated from microarray experiments. Genes were selected based on a high level of differential gene expression in one or more cell line – time point combinations, an important role in a biological pathway/network relevant to cancer or inflammation, or effects on epigenetics.

Gene expression was measured using qRT-PCR in the following genes: *AREG*, *ARID5B*, *CDKN2B*, *CYP1B1*, *CYP51A1*, *DHCR7*, *DUSP10*, *EGFR*, *EPGN*, *IFIT2*, *HMGCR*, *HMGCS1*, *GULP1*, *IDI1*, *INSIG1*, *KRT17*, *LDLR*, *MMP1*, *MMP3*, *NR4A3*, *PTGS2*, *RSG4*, *SCD*, *SGK2*, *SQLE*, *TM7SF2* and *TP53INP1* (Supplementary Table 1). The aforementioned genes were selected based on the level of differential gene expression and relevance to cancer/epigenetic mechanisms. Although the magnitude of change varied between the two methods with qRT-PCR generating the higher value in general, the direction of change remained consistent, with the exception of the gene *ARID5B*. The gene expression level of *ARID5B* was down-regulated according to the results obtained from the Affymetrix array (fold change of -1.82), and up-regulated according to the results generated by qRT-PCR (fold change of 1.43).

*GAPDH* and *HPRT1* were used as normalisation genes as they showed consistent results in both PC3 and DU145 cell lines across the Ct range of the 27 genes tested. Following normalisation, the fold changes in expression of the selected genes were compared between those generated from the Affymetrix microarray and those generated from qRT-PCR experiments (Supplementary Table 1).

### 3.3 GATHER

GATHER software was used to analyse the relationships between individual or groups of genes. Only those genes that were differentially expressed with a p-value  $\leq 0.05$  and a minimum fold change of 1.5 were uploaded to GATHER. SN30028 treatment modulated biological processes and the involved genes are summarised in Supplementary Table 2. Those biological processes with Bayes factors  $\geq 3$  and p-values  $\leq 0.05$  were nominated<sup>32</sup>. The Gene Ontology (GO) database was used to obtain definitions of biological processes.<sup>33</sup>

The biological processes with the highest Bayes factors following treatment of PC3 cells with SN30028 at 4, 24 and 96 hours were: the transforming growth factor beta receptor signalling process (3.53), cyclooxygenase process (4.72), and response to nutrients process (5.69), respectively. In DU145 cells the sterol biosynthesis and sterol metabolism processes had the highest Bayes factors at 4 (29.66 and 26.51 respectively) and 24 hours (51.26 and 49.75 respectively), and cell proliferation and cell cycle were the most affected biological processes at 96 hour (25.21 and 21.49 respectively) following SN30028 treatment.

### 3.4 Ingenuity Pathways Analysis

IPA software (IPA<sup>®</sup>, QIAGEN Redwood City, USA) was used to transform a list of genes into a set of relevant networks<sup>29</sup> and this software is widely used for biological pathway, function and disease, and molecular network analysis.<sup>34,35</sup> All results from each time-point-cell line combination were submitted to IPA with the filters and settings as follows: adjusted p-value of 0.05 and fold-change of 1.5. The most significantly affected canonical pathways and diseases in response to treatment by SN30028 at three time points in PC3 and DU145 cell lines generated through IPA are shown in Table 4. Using Fischer's exact test, the results were ranked. The ratios listed in the table represent the number of genes in the dataset that were in the canonical pathway stated, divided by the total number of genes in that particular pathway.

Table 4. The top canonical pathways, diseases and functions affected by SN30028 treatment at three time points in PC3 and DU145 cell lines

PC3	Top canonical pathways	p-value	Differentially expressed genes*	Ratio
4 hours	Glucocorticoid receptor signalling	2.76E-04	BCL2, CSF2, NCOR2, MMP1, PTGS2	7/272
	Docosahexaenoic acid (DHA) signalling	7.88E-04	BCL2, BIK, FOXO1	3/39
	Chondroitin sulfate degradation	1.61E-03	HEXA, MGEA5	2/13
	Dermatan sulfate degradation	1.88E-03	HEXA, MGEA5	2/14
	PI3K/AKT signalling	2.46E-03	BCL2, FOXO1, GDF15, PTGS2	4/121
	<b>Associated network functions</b>			<b>Score</b>

	Developmental disorder, cell death and survival, organismal injury and abnormalities.			60
	Cellular growth and proliferation, cell death and survival, cancer.			56
	Cellular development, cellular growth and proliferation, haematological system development and function.			37
	Post-translational modification, cancer, gastrointestinal disease.			2
	Cell morphology, cellular function and maintenance, DNA replication, recombination, and repair.			2
<b>PC3</b>	<b>Top canonical pathways</b>	<b>p-value</b>	<b>Differentially expressed genes*</b>	<b>Ratio</b>
<b>24 hours</b>	Role of IL-17A in arthritis	5.43E-04	MMP1, PTGS2	2/54
	Zymosterol biosynthesis	3.89E-03	MSMO1	1/6
	Airway pathology in chronic obstructive pulmonary disease	5.18E-03	MMP1	1/8
	Prostanoid biosynthesis	5.83E-03	PTGS2	1/9
	Cholesterol biosynthesis I	8.41E-03	MSMO1	1/13
	<b>Associated network functions</b>			<b>Score</b>
	Cancer, dermatological diseases and conditions, tissue morphology.			38
<b>PC3</b>	<b>Top canonical pathways</b>	<b>p-value</b>	<b>Differentially expressed genes*</b>	<b>Ratio</b>
<b>96 hours</b>	Unfolded protein response	1.52E-04	DDIT3, DNAJB9, HSPA5, INSIG1	4/53
	Superpathway of cholesterol biosynthesis	3.41E-04	ACAT2, HMGCS1, SQLE	3/27
	Ketogenesis	1.12E-03	ACAT2, HMGCS1	2/10
	Mevalonate pathway I	1.63E-03	ACAT2, HMGCS1	2/12
	Superpathway of geranylgeranyl-diphosphate biosynthesis I	2.93E-03	ACAT2, HMGCS1	2/16
	<b>Associated network functions</b>			<b>Score</b>
	Cancer, organismal injury and abnormalities, neurological disease.			46
	Cardiovascular disease, hereditary disorder, metabolic disease.			30
	Lipid metabolism, molecular transport, small molecule biochemistry.			30
	Cell-to-cell signalling and interaction, cellular assembly and organization, cellular function and maintenance.			30
	Cancer, endocrine system disorders, organismal injury and abnormalities.			28
<b>DU145</b>	<b>Top canonical pathways</b>	<b>p-value</b>	<b>Differentially expressed genes*</b>	<b>Ratio</b>
<b>4 hours</b>	Superpathway of cholesterol biosynthesis	4.03E-15	HMGCR, MSMO1, MVK, SC5D, SQLE	8/27
	Cholesterol biosynthesis I	1.66E-10	DHCR7, MSMO1, NSDHL, SC5D, SQLE	5/13
	Cholesterol biosynthesis II	1.66E-10	DHCR7, MSMO1, NSDHL, SC5D, SQLE	5/13
	Cholesterol biosynthesis III	1.66E-10	DHCR7, MSMO1, NSDHL, SC5D, SQLE	5/13

	Mevalonate pathway I	4.28E-06	HMGCR, HMGCS1, MVK	3/12
	<b>Associated network functions</b>			<b>Score</b>
	Cancer, cell morphology, cellular function and maintenance.			43
	Cardiovascular disease, metabolic disease, lipid metabolism.			35
	Drug metabolism, small molecule biochemistry, cellular assembly and organization.			35
<b>DU145</b>	<b>Top canonical pathways</b>	<b>p-value</b>	<b>Differentially expressed genes*</b>	<b>Ratio</b>
	Superpathway of cholesterol biosynthesis	3.25E-32	HMGCS1, MSMO1, SC5D, HSD17B7, SQLE	17/27
<b>24 hours</b>	Cholesterol biosynthesis I	1.53E-23	MSMO1, SC5D, HSD17B7, SQLE, TM7SF2	11/13
	Cholesterol biosynthesis II	1.53E-10	MSMO1, SC5D, HSD17B7, SQLE, TM7SF2	11/13
	Cholesterol biosynthesis III	1.53E-10	MSMO1, SC5D, HSD17B7, SQLE, TM7SF2	11/13
	Zymosterol biosynthesis	4.07E-06	CYP51A1, HSD17B7, MSMO1, NSDHL, TM7SF2	5/6
	<b>Associated network functions</b>			<b>Score</b>
	Lipid metabolism, small molecule biochemistry, vitamin and mineral metabolism.			66
	Carbohydrate metabolism, lipid metabolism, small molecule biochemistry.			63
	Lipid metabolism, small molecule biochemistry, vitamin and mineral metabolism.			60
	Antimicrobial response, inflammatory response, infectious disease.			23
<b>DU145</b>	<b>Top canonical pathways</b>	<b>p-value</b>	<b>Differentially expressed genes*</b>	<b>Ratio</b>
	Molecular mechanisms of cancer	7.24E-07	RHOA, CDH1, SHC1, BBC3, PLCB4	46/359
<b>96 hours</b>	Cell cycle control of chromosomal replication I	1.75E-06	ORC6, CDC6, CDT1, CDC45, MCM2	10/27
	Estrogen-mediated S-phase entry	5.18E-06	CCNE2, CDKN1B, E2F5, CCND1, CDK1	9/24
	Glioblastoma multiforme signaling I	1.49E-05	RHOA, SHC1, PLCB4, PLCB1, PTEN	23/145
	Glioma signaling	3.45E-05	SHC1, PTEN, IGF1R, PRKCA, PA2G4	17/94
	<b>Associated network functions</b>			<b>Score</b>
	Skeletal and muscular system development and function, protein synthesis, cellular compromise.			84
	Cellular development, cellular growth and			77

proliferation, digestive system development and function.	
Post-translational modification, cell cycle, hair and skin development and function.	73
Cell cycle, cellular assembly and organization, DNA replication, recombination, and repair.	68
DNA replication, recombination, and repair, cell cycle, connective tissue disorders.	67

---

Ratio = differentially expressed genes/total number of genes in that pathway

\* = up to five genes with the smallest p-values were selected

Obtaining a list of genes and related pathways is informative, but it is the identification of the connections between the pathways that is important. The IPA networks are assembled based on connectivity between genes. Several networks were generated by IPA software from each microarray experiment using the IPA knowledge base, but only the strongest network for each cell line – time point combination are shown here (Supplementary Figures 1-6). The genes in the network are associated with numerous diseases and disease related functions, which are listed according to p-values or score (Table 4). The scores of the IPA network indicate how relevant the network is to the genes in the uploaded dataset (Score =  $-\log_{10}$  (p-value)). It is evident from Table 4 that cancer-related pathways are highly affected by SN30028 treatment in both cell lines. The parameters were set at either 70 or 35 molecules per network and a direct interaction between the molecules. Only relevant genes with an adjusted p-value < 0.05 and fold change > 1.5 or < -1.5 were selected for network analysis.

IPA generated results regarding the most prominent diseases and functions associated with the network depicted in Figures 3-8. These diseases and functions included developmental disorders, cancer, inflammatory disorders, cell death and survival, cellular growth and proliferation, cellular function and maintenance and DNA replication amongst others. Using the Fisher's exact test IPA calculates a network score which is the  $\log_{10}$  of the p-value of the network.<sup>29</sup> The network scores ranged from 38 (Supplementary Figure 2) to 84 (Supplementary Figure 6) and between 13% (Supplementary Figure 2) and 100% (Supplementary Figure 6) of the genes in each network were differentially expressed.

#### 4 Discussion

Regulation of gene expression is encoded by the genome and by the epigenome. The focus of this discussion is on the modulation of gene expression and the molecular interaction of differentially expressed genes, represented in the form of networks, generated using transcriptomics and analysed using IPA. The most common pathways, as shown in Table 4, will be examined. Similarly, central nodes in networks will be discussed if they are evident in more than one network.

Novel compounds were used to treat prostate cancer cell lines, inhibition of cell proliferation was observed and HDAC activity was assessed to determine which compound-cell line combination to use in the transcriptomics experiments. DU145 was found to be more tolerant to the novel compounds than PC3 and LNCaP, and LNCaP was found to be the most sensitive to the novel compounds with respect to cell proliferation. In contrast, DU145 had the greatest response to the novel compounds with respect to HDAC inhibition, whereas LNCaP had the least or no inhibitory response to these

compounds. In addition, there was a far greater response observed in DU145 than in PC3 when considering the number of genes differentially expressed, as well as the size of the response.

There are a number of phenotypic and genotypic differences amongst PC3, DU145 and LNCaP. LNCaP is androgen sensitive, whilst PC3 and DU145 are androgen independent. HDAC inhibitors interfere with androgen receptor activity<sup>36</sup> and therefore it is likely that the cell lines would respond differently. Seeing that PC3 and DU145 are androgen independent, it was not surprising that a change in the *AR gene* was not observed.

In addition to androgen sensitivity, the three cell lines of interest also differ with regards to TNF $\beta$ . When treated with TNF $\beta$ , cell proliferation was initially inhibited, whilst no effect was observed in LNCaP cells.<sup>37</sup> TGF $\beta$  induces epigenetic changes to modulate cell proliferation, differentiation and migration, and that TGF $\beta$  may initiate cellular changes that facilitate its role as both a tumour suppressor during the early stages of tumour development, and as a tumour promoter in metastatic or later stage disease.<sup>5</sup> HDAC inhibitors may inhibit the activation of TGF $\beta$  in epithelial cells<sup>5</sup> by blocking TGF $\beta$  mediated epithelial-mesenchymal transition (EMT), which is essential for cell growth and invasion.<sup>38</sup> In our study we found that TGF $\beta$  was down regulated in response to SN30028, with fold changes between 1.074 and 1.707 (adjusted p values were significant for DU145 96hr treatment only).

#### 4.1 Biological Processes and Pathways

Based on the transcriptomics results and analysis using GATHER and IPA, a number of cancer related “biological processes,” “diseases and disorders” and “network associated functions” were affected by SN30028 treatment of the prostate cancer cell lines, DU145 and PC3 at all three time points tested (Table 4). Using GATHER, the most commonly modulated biological processes in DU145 (with high Bayes factor values) were in relation to sterol and cholesterol metabolism and biosynthesis (Supplementary Table 2) at the 4 and 24 hr time points, whilst at 96 hrs the more directly cancer related biological processes of cell proliferation, cell cycle and DNA replication were evident. This is consistent with data generated using IPA. The top canonical pathways generated using IPA included those related to cholesterol biosynthesis (PC3 – 24 and 96 hrs, and DU145 – 4 and 24hrs) and the mevalonate pathway (PC3 – 96hrs and DU145 – 4hrs).

Other studies have been carried out using gene expression arrays, or targeted gene expression to assess levels of gene expression in normal versus adenocarcinoma or precursor adenocarcinoma tissues as well as in cell lines in response to HDAC inhibitors.<sup>39-43</sup> Variations were observed in different cancer cell lines in response to HDAC inhibitors, with, in some cases, non-overlapping cellular targets.<sup>43</sup> Using different cell lines and a different HDAC inhibitor, it is not surprising that different pathways were modulated, although some overlap was observed with respect to modification of gene expression.

Cholesterol metabolism plays an important role in providing cells with compounds for growth and sterol biosynthesis is an essential metabolic component of cancers.<sup>44</sup> In addition, overexpression of cholesterol biosynthesis pathways has been previously detected in refractory breast cancers<sup>45</sup> and this is consistent with the data observed from the metastatic prostate cancer cell lines we tested. More specifically, *cytochrome P450 1B1 (CYP1B1)* is important for the synthesis of cholesterol steroids and lipids, and is well known for its role in drug metabolism.<sup>46</sup> *CYP1B1* activity is inhibited by a number of anti-cancer agents and is commonly over-expressed in variety of tumours.<sup>47</sup> In our study the expression of *CYP1B1* was down regulated in PC3 cells treated for 4 and 24hrs, and it is suggested that the inhibition of *CYP1B1* is brought about through the inhibition of HDAC6 activity.<sup>48</sup> In contrast, inconsistencies have arisen, for example the HDAC inhibitors SAHA and TSA induced *CYP1B1* expression in the human breast cancer MCF-7.<sup>49</sup>



The mevalonate pathway has a broad influence and is associated with the cholesterol related biosynthesis pathways; is important in cellular metabolism; plays a role in the maintenance of cell membranes; is involved in steroid biosynthesis and can be disrupted by medication prescribed for bone-density disorders and high cholesterol levels.<sup>50, 51</sup> In addition, the mevalonate pathway is an important target for anti-cancer therapy and inhibitors of this pathway target malignant cell growth<sup>50, 51</sup> and are believed to act through the modification of methylation status of CpG sites in gene promoter regions involved in apoptosis and/or cell proliferation.<sup>52</sup> In addition, DU145 cells, after 96 hours of treatment, showed the top canonical pathway affected was “molecular mechanisms of cancer” with 46 of the 359 genes involved were differentially expressed.

All cell line – treatment time combinations showed cancer to be one of the top five diseases and disorders, with the exception of DU145 at 24hrs with a closely related disease/disorder, namely inflammatory response listed in the top five. The number of cancer related genes that were differentially expressed for each cell line - treatment time combination ranged from 11 to 445 genes with p values ranging from 8.00E-02 to 2.15E-17. It is clear that numerous cancer related genes were differentially expressed in prostate cancer cell lines in response to treatment and therefore the compound, SN30028 is of interest. Similarly, Chang et al. found that a large number of genes were differentially expressed in response to the HDAC inhibitor, TSA, in non-small cell lung cancer.<sup>43</sup> However, in the study by Chang et al,<sup>43</sup> the fold-changes observed were much higher than those reported here.

“Associated network functions” were also listed as an output from IPA for each cell line – treatment time combination. Cell cycle, cellular growth and proliferation, DNA replication and repair, inflammatory response, and cancer all ranked highly in one or more of the cell line – treatment time combinations and thus it is evident that SN30028 has an impact on cancer related mechanisms.

## 4.2 Networks

The networks shown in Supplementary Figures 1 and 2 demonstrate that *prostaglandin H synthase (PTGS2)*, otherwise known as *COX2*, connects with many genes in networks generated from PC3 treated for 4 and 24 hours and was one of the top ten differentially expressed genes following PC3 treatment for 4hrs (Table 2). The down regulation of *COX2* was corroborated in qRT-PCR experiments (Supplementary Table 1). *COX2* is down-regulated by treatment with SN30028 for 4 and 24 hours (PC3) by a fold change of -1.71 and -2.47 respectively. *COX2* plays a key role in prostanoid production by catalysing the conversion of arachidonic acid to prostaglandin G2 and H2 resulting in an inflammatory response.<sup>53, 54</sup> Numerous studies have been conducted to investigate *COX2* inhibition and the reduction in inflammatory response<sup>55</sup> and its role in oncogenesis.<sup>56</sup> Non-steroidal anti-inflammatory drugs are a class of drugs that inhibit *COX2* enzyme activity and thereby reduce the inflammatory response.<sup>57, 58</sup> This supports the notion that SN30028 has anti-inflammatory effects.

*Matrix metalloproteinase 3 (MMP3)* was initially up-regulated in PC3 cells treated with SN30028 (Table 2, Supplementary Figure 1), but this response was not maintained. In addition, although *MMP3* acts on a number of different genes, the expression of these genes was not modified when *MMP3* was up-regulated (Supplementary Figure 1). Although *MMP3* is over-expressed in most human cancers, and is known to induce initial cancer cell-growth and differentiation, rather than act at a later stage in cancer progression<sup>59, 60</sup>, it is also known to have many opposing functions<sup>59</sup> and to date *MMP* inhibitors have not been successful in the clinic.<sup>60</sup>

Differential expression of numerous other central node or core genes is evident, but none of the central node genes arise in more than two top ranked networks representing each cell line - treatment time combination. Some of the differentially expressed central node genes include *FOXO1* and 3, thought to be involved in triggering apoptosis or cell survival and are induced by oxidative stress;<sup>61</sup> *amphiregulin (AREG)* was down-regulated in PC3 (Supplementary Figures 2 and 3) supporting the idea that SN30028 reduces inflammation and inhibits tumour development.<sup>62</sup> AREG is a ligand of *epidermal growth factor receptor (EGFR)*<sup>62</sup> and the fact that *EGFR* is up-regulated in DU145 (Supplementary Figure 4) could either be a chance occurrence as this finding was only attained in DU145 treated for 4hrs and therefore is an initial response that is not sustained, or it could be that SN30028 works through different mechanisms in the two cell lines. Up-regulation of *EGFR* is associated with prostate cancer progression and *EGFR* dysfunction induces cell survival, proliferation, invasion and metastasis and therefore was not an anticipated response. The *AR* gene is known to interact with *EGFR* and we wouldn't expect to see a change in expression as DU145 and PC3 are androgen insensitive. However, although these cell lines are regarded as androgen non-responsive, some authors have reported low level expression of AR mRNA, and treatment with interferon (IFN) resulted in up-regulation of AR protein levels.<sup>63</sup> This may be due to AR phosphorylation. In the experiments reported herein a change in AR expression in response to treatment with SN30028 was not noted.

Similar to the unexpected up-regulation of *EGFR*, the *ETS-related gene (ERG)* was up-regulated (at low intensity) after 96hrs (Figure 8) and is an unexpected response. *ERG* is a proto-oncogene, regulates cell proliferation, differentiation, angiogenesis, inflammation, apoptosis and can result in gene fusion products associated with prostate and other cancers.<sup>64</sup> *ERG*, when over-expressed, is able to regulate oncogenic pathways involving *cMyc*, *AR* and *EZH2*,<sup>64</sup> none of which were up-regulated in this study. *ERG* acts on *neuronally expressed developmentally down-regulated 4 (NEDD4)*,<sup>64</sup> which is a central node gene that was down-regulated in DU145 cells (Supplementary Figure 6). NEDD4 is an oncoprotein that promotes degradation through the ubiquitination of its substrates and it is also thought to promote colon and lung carcinogenesis, be over-expressed in prostate, breast and bladder cancers, and promotes growth of colon cancer cells independently of PTEN and PI3K/AKT signalling.<sup>65</sup> Despite the fact that *ERG* is over-expressed in DU145 after 96hrs of treatment and acts on *NEDD4* (amongst other genes), SN30028 appears to inhibit *NEDD4* which is desirable, although further work is required for the elucidation of the mechanisms involved in treating cancers in this way.

## 5 Conclusions

In conclusion SN30028, an HDAC inhibitor was synthesised and used in the treatment of prostate cancer cell lines for 4, 24 and 96 hrs, and assessed for differential gene expression. Using IPA software the data were analysed and pathways involved in cholesterol biosynthesis and mevalonate were affected most commonly in the cell line DU145. In addition to pathway and network analysis the most frequently affected diseases and disorders were assessed. Those related to inflammatory response and/or cancers were one of the top five diseases and disorders listed for each cell line-time point tested. SN30028 showed it could be a potential therapeutic agent in treating prostate cancer by targeting the sterol and mevalonate pathways, however further work is required to confirm these results.

## Acknowledgements

Liam Williams is acknowledged for performing the microarray assays and Daniel Hurley carried out the statistical analysis and normalisation of the Affymetric data (New Zealand Genomics Limited, Auckland, New Zealand). Matthew Barnett (AgResearch Ltd, Palmerston North, New Zealand) provided guidance on the use of IPA software.

## Funding

This work was funded by the Auckland Cancer Society Research Centre.

## 6 References

1. C. N. Serhan, *The Journal of the Federation of American Societies for Experimental Biology*, 2011, **25**, 1441-1448.
2. C. H. Arrowsmith, C. Bountra, P. V. Fish, K. Lee and M. Schapira, *Nature Reviews Drug Discovery* 2012, **11**, 384-400.
3. N. Dali-Youcef, S. Froelich, F.-M. Moussallieh, S. Chibbaro, G. Noël, I. J. Namer, S. Heikkinen and J. Auwerx, *Sci Rep-Uk*, 2015, **5**.
4. O. Khan and N. B. La Thangue, *Immunology and cell biology*, 2012, **90**, 85-94.
5. M. Pickup, S. Novitskiy and H. L. Moses, *Nature Reviews Cancer*, 2013, **13**, 788-799.
6. J. E. Bolden, M. J. Peart and R. W. Johnstone, *Nature reviews. Drug discovery*, 2006, **5**, 769-784.
7. Z. Lin, P. M. Murray, Y. Ding, W. A. Denny and L. R. Ferguson, *Mutation Research*, 2010, **7**;;, 81-88.
8. Z. W. Lin, Master of Health Sciences, University of Auckland, 2009.
9. Z. W. Lin, PhD, University of Auckland, 2015.
10. A. J. de Ruijter, A. H. van Gennip, H. N. Caron, S. Kemp and A. B. van Kuilenburg, *The Biochemical Journal*, 2003, **370**, 737-749.
11. G. Lagger, D. O'Carroll, M. Rembold, H. Khier, J. Tischler, G. Weitzer, B. Schuettengruber, C. Hauser, R. Brunmeir, T. Jenuwein and C. Seiser, *The EMBO Journal*, 2002, **21**, 2672-2681.
12. U. Mahlknecht, J. Will, A. Varin, D. Hoelzer and G. Herbein, *Journal of Immunology*, 2004, **173**, 3979-3990.
13. C. Boyault, Y. Zhang, S. Fritah, C. Caron, B. Gilquin, S. H. Kwon, C. Garrido, T. P. Yao, C. Vourc'h, P. Matthias and S. Khochbin, *Genes & Development*, 2007, **21**, 2172-2181.
14. G. I. Aldana-Masangkay and K. M. Sakamoto, *Journal of Biomedicine and Biotechnology*, 2011, **2011**, 10.
15. G. Marlow, S. Ellett, I. R. Ferguson, S. Zhu, N. Karunasinghe, A. C. Jesuthasan, D. Y. Han, A. G. Fraser and L. R. Ferguson, *Human Genomics*, 2013, **7**, 24.
16. Affymetrix, GeneChip® PrimeView™ Human Gene Expression Array Datasheet, [http://media.affymetrix.com/support/technical/datasheets/primeview\\_array\\_cartridge\\_datasheet.pdf](http://media.affymetrix.com/support/technical/datasheets/primeview_array_cartridge_datasheet.pdf), (accessed 4 Aug 2015).
17. Q. Li, N. J. Birkbak, B. Györfy, Z. Szallasi and A. C. Eklund, *BioMed Central Bioinformatics*, 2011, **12**.
18. J. T. Chang, C. Carvalho, S. Mori, A. H. Bild, M. L. Gatzka, Q. Wang, J. E. Lucas, A. Potti, P. G. Febbo, M. West and J. R. Nevins, *Molecular Cell*, 2009, **34**, 104-114.
19. A. G. Wilson, *Journal of periodontology*, 2008, **79**, 1514-1519.
20. P. Skehan, R. Storeng, D. Scudiero, A. Monks, J. McMahon, D. Vistica, J. T. Warren, H. Bokesch, S. Kenney and M. R. Boyd, *Journal of the National Cancer Institute*, 1990, **82**, 1107-1112.
21. F. J. Staal, M. van der Burg, L. F. Wessels, B. H. Barendregt, M. R. Baert, C. M. van den Burg, C. van Huffel, A. W. Langerak, V. H. van der Velden, M. J. Reinders and J. J. van Dongen, *Leukemia*, 2003, **17**, 1324-1332.
22. H. Auer, D. L. Newsom and K. Kornacker, *Methods in Molecular Biology*, 2009, **509**, 35-46.
23. C. H.-J. Kao, K. S. Bishop, D. Y. Han, P. M. Murray, M. P. Glucina, G. J. Marlow and L. R. Ferguson, *Functional Foods in Health and Disease*, 2014, **4**, 182-207.
24. J. S. Yuan, A. Reed, F. Chen and C. N. Stewart, Jr., *BMC bioinformatics*, 2006, **7**, 85.
25. R. A. Irizarry, B. Hobbs, F. Collin, Y. D. Beazer - Barclay, K. J. Antonellis, U. Scherf and T. P. Speed, *Biostatistics*, 2003, **4**, 249-264.
26. R. F. f. S. Computing, R: A language and environment for statistical computing. , <http://www.R-project.org>).

27. Y. Benjamini and Y. Hochberg, *Journal of the Royal Statistical Society Series B (Methodological)*, 1995, **57**, 289-300.
28. J. Chang and J. Nevins, *Bioinformatics*, 2006, **22**, 2926-2933.
29. IPA, *White Paper: IPA Network Generation Algorithm*, 2005.
30. F. Long, H. Liu, C. Hahn, P. Sumazin, M. Zhang and A. Zilberstein, *In Silico Biol.*, 2004, **4**, 0033.
31. J. Vandesompele, K. De Preter, F. Pattyn, B. Poppe, N. Van Roy, A. De Paepe and F. Speleman, *Genome biology*, 2002, **3**, RESEARCH0034.
32. R. E. Kass and A. E. Raftery, *Journal of the American Statistical Association*, 1995, **90**, 773-795.
33. M. Ashburner, C. A. Ball, J. A. Blake, D. Botstein, H. Butler, J. M. Cherry, A. P. Davis, K. Dolinski, S. S. Dwight, J. T. Eppig, M. A. Harris, D. P. Hill, L. Issel-Tarver, A. Kasarskis, S. Lewis, J. C. Matese, J. E. Richardson, M. Ringwald, G. M. Rubin and G. Sherlock, *Nature Genetics*, 2000, **25**, 25-29.
34. H. Lv, L. Liu, Y. Zhang, T. Song, J. Lu and X. Chen, *Molecular bioSystems*, 2010, **6**, 2056-2067.
35. G. Marlow, S. Ellett, I. R. Ferguson, S. Zhu, N. Karunasinghe, A. C. Jesuthasan, D. Y. Han, A. G. Fraser and L. R. Ferguson, *Human genomics*, 2013, **7**, 24.
36. D. S. Welsbie, J. Xu, Y. Chen, L. Borsu, H. I. Scher, N. Rosen and C. L. Sawyers, *Cancer Research*, 2009, **69**, 958-966.
37. G. Wilding, G. Zugmeier, C. Knabbe, K. Flanders and E. Gelmann, *Molecular and Cellular Endocrinology*, 1989, **62**, 79-87.
38. E. Smolle, V. Taucher, E. Petru and J. Haybaeck, *Anticancer Res.*, 2014, **34**, 1519-1530.
39. N. Sato, H. Matsubayashi, T. Abe, N. Fukushima and M. Goggins, *Clinical Cancer Research*, 2005, **11**, 4681-4688.
40. E. Capobianco, A. Mora, D. La Sala, A. Roberti, N. Zaki, E. Badidi, M. Taranta and C. Cinti, *PLoS ONE*, 2014, **9**, e95596.
41. F. Wisniewski, D. Calcagno, M. Leal, E. Chen, C. Gigeck, L. Santos, T. Pontes, L. Rasmussen, S. Payão, P. Assumpção, L. Lourenço, S. Demachki, R. Artigiani, R. Burbano and M. Cardoso Smith, *Tumor Biol*, 2014, **35**, 6373-6381.
42. N. Mahmud, B. Petro, S. Baluchamy, X. Li, S. Taioli, D. Lavelle, J. G. Quigley, M. Suphangul and H. Araki, *Biol Blood Marrow Tr*, 2014, **20**, 480-489.
43. J. Chang, D. S. Varghese, M. C. Gillam, M. Peyton, B. Modi, R. L. Schiltz, L. Girard and E. D. Martinez, *British Journal of Cancer*, 2012, **106**, 116-125.
44. A. Gorin, L. Gabitova and I. Astsaturov, *Current Opinion in Pharmacology*, 2012, **12**, 710-716.
45. S. P. Pitroda, N. N. Khodarev, M. A. Beckett, D. W. Kufe and R. R. Weichselbaum, *P Natl Acad Sci USA*, 2009, **106**, 5837-5841.
46. P. B. Danielson, *Current drug metabolism*, 2002, **3**, 561-597.
47. H. Piotrowska, M. Kucinska and M. Murias, *Molecular and cellular biochemistry*, 2013, **383**, 95-102.
48. V. D. Kekatpure, A. J. Dannenberg and K. Subbaramaiah, *The Journal of Biological Chemistry*, 2009, **284**, 7436-7445.
49. L. A. Hooven, B. Mahadevan, C. Keshava, C. Johns, C. Pereira, D. Desai, S. Amin, A. Weston and W. M. Baird, *Bioorganic & Medicinal Chemistry Letters*, 2005, **15**, 1283-1287.
50. A. Ilyas, Z. Hashim, N. Naeem, K. Haneef and S. Zarina, *Int J Proteomics*, 2014, **Article ID 532953**.
51. K. M. Swanson and R. J. Hohl *Current Cancer Drug Targets*, 2006, **6**, 15-37.
52. R. Thaler, S. Spitzer, H. Karlic, C. Berger, K. Klaushofer and F. Varga, *Biochemical Pharmacology*, 2013, **85**, 173-185.
53. E. Ricciotti and G. A. FitzGerald, *Arteriosclerosis, thrombosis, and vascular biology*, 2011, **31**, 986-1000.
54. W. L. Smith, D. L. DeWitt and R. M. Garavito, *Annual Review of Biochemistry*, 2000, **69**, 145-182.

55. H. Yokouchi, K. Kanazawa, T. Ishida, S. Oizumi, N. Shinagawa, N. Sukoh, M. Harada, S. Ogura, M. Munakata, H. Dosaka-Akita, H. Isobe and M. Nishimura, *Mol Clin Oncol*, 2014, **2**, 744-750.
56. I. Stasinopoulos, T. Shah, M. F. Penet, B. Krishnamachary and Z. M. Bhujwalla, *Frontiers in Pharmacology*, 2013, **4**, 34.
57. C. Luong, A. Miller, J. Barnett, J. Chow, C. Ramesha and M. F. Browner, *Nature structural biology*, 1996, **3**, 927-933.
58. M. Annamanedi and A. M. Kalle, *PLoS One*, 2014, **9**, e99285.
59. M. D. Sternlicht, A. Lochter, C. J. Sympson, B. Huey, J. P. Rougier, J. W. Gray, D. Pinkel, M. J. Bissell and Z. Werb, *Cell*, 1999, **98**, 137-146.
60. J. Cathcart, A. Pulkoski-Gross and J. Cao, *Genes Dis*, 2015, **1**, 26-34.
61. R. C. Poulsen, A. J. Carr and P. A. Hulley, *Biochemical and Biophysical Research Communications*, 2015, **462**, 78-84.
62. C. Berasain and M. A. Avila, *Seminars in cell & developmental biology*, 2014, **28**, 31-41.
63. F. Alimirah, J. Chen, Z. Basrawala, H. Xin and D. Choubey, *Federation of European Biochemical Societies Letters*, 2006, **580**, 2294-2300.
64. L. Wu, J. C. Zhao, J. Kim, H.-J. Jin, C.-Y. Wang and J. Yu, *Cancer Research*, 2013, **73**, 6068-6079.
65. X. Ye, L. Wang, B. Shang, Z. Wang and W. Wei, *Current Cancer Drug Targets*, 2014, **14**, 549-556.

**Supplementary Figure 1.** A biological network of genes related to cancer following the treatment of PC3 cells with SN30028 (4-hour). The network was generated using the Ingenuity Pathway Analysis software. Genes represented by a red node were up-regulated and those represented by a green node were down-regulated. Increasing colour intensity represents increasing differential gene expression. The nodes with an asterisk at the right of the name of the gene indicate that the gene is represented by more than one probe in the array.

**Supplementary Figure 2.** A biological network of genes related to cancer following the treatment of PC3 cells with SN30028 (24-hour). The network was generated using the Ingenuity Pathway Analysis software. Genes represented by a red node were up-regulated and those represented by a green node were down-regulated. Increasing colour intensity represents increasing differential gene expression. The nodes with an asterisk at the right of the name of the gene indicate that the gene is represented by more than one probe in the array.

**Supplementary Figure 3.** A biological network of genes related to cancer following the treatment of PC3 cells with SN30028 (96-hour). The network was generated using the Ingenuity Pathway Analysis software. Genes represented by a red node were up-regulated and those represented by a green node were down-regulated. Increasing colour intensity represents increasing differential gene expression. The nodes with an asterisk at the right of the name of the gene indicate that the gene is represented by more than one probe in the array.

**Supplementary Figure 4.** A biological network of genes related to cancer following the treatment of DU145 cells with SN30028 (4-hour). The network was generated using the Ingenuity Pathway Analysis software. Genes represented by a red node were up-regulated and those represented by a green node were down-regulated. Increasing colour intensity

represents increasing differential gene expression. The nodes with an asterisk at the right of the name of the gene indicate that the gene is represented by more than one probe in the array.

**Supplementary Figure 5.** A biological network of genes related to cancer following the treatment of DU145 cells with SN30028 (24-hour). The network was generated using the Ingenuity Pathway Analysis software. Genes represented by a red node were up-regulated and those represented by a green node were down-regulated. Increasing colour intensity represents increasing differential gene expression. The nodes with an asterisk at the right of the name of the gene indicate that the gene is represented by more than one probe in the array.

**Supplementary Figure 6.** A biological network of genes related to cancer following the treatment of DU145 cells with SN30028 (96-hour). The network was generated using the Ingenuity Pathway Analysis software. Genes represented by a red node were up-regulated and those represented by a green node were down-regulated. Increasing colour intensity represents increasing differential gene expression. The nodes with an asterisk at the right of the name of the gene indicate that the gene is represented by more than one probe in the array.